Electron, muon, and nuclear spin dynamics in $SmRh_4B_4$ and $ErRh_4B_4$

D. R. Noakes, J. H. Brewer, and D. R. Harshman*
TRIUMF and Department of Physics, University of British Columbia, Vancouver, B.C., Canada V6T 2A3

E. J. Ansaldo
Department of Physics, University of Saskatchewan, Saskatoon, Saskatchewan, Canada S7N 0W0

C. Y. Huang
Los Alamos National Laboratory, Los Alamos, New Mexico 87544
(Received 17 November 1986)

Zero-field positive muon spin relaxation (ZF-μ^+SR) studies of $SmRh_4B_4$ and $ErRh_4B_4$ have revealed several features of magnetic moment dynamics in these magnetic superconductors. The shape of the μSR signal is not simple over most of the temperature range studied in either $SMRh_4B_4$ or $ErRh_4B_4$ because of the complicated nature of both materials. In $SmRh_4B_4$ above 200 K we observe complete decoupling of the muon spins from the stable, localized samarium ionic moments due to the extremely fast fluctuation of those moments; below 200 K there is a nearly simultaneous onset of coupling of the samarium electronic moments to both the muon spins and the ^{11}B nuclear moments. The muon spin-relaxation rate in $SmRh_4B_4$ increases smoothly as the temperature is lowered through the superconducting transition toward the antiferromagnetic ordering at 0.87 K. In $ErRh_4B_4$ the muon spin-relaxation function is a sum of two exponentials down to 50 K, below which the relaxation becomes too fast to be detected by our instruments, leaving only a signal of much-reduced amplitude at lower temperatures. We attribute the two exponentials to two distinct types of muon site in the crystal structure: a (high rms field) channel structure around the rare earths, and a (low rms field) site at the center of the RhB cluster. The deduced fluctuation rates of the rare-earth dipole fields at the muons are generally consistent with a model of paramagnetic rare-earth fluctuation mechanisms (Ruderman-Kittel-Kasuya-Yosida, Korringa, and spin-lattice interactions) above 4 K in $SmRh_4B_4$ and above 50 K (i.e., where the signal is fully resolved) in $ErRh_4B_4$. Below 4 K in $SmRh_4B_4$, there is excess relaxation that seems to be associated with the magnetic ordering and that cannot be explained by the model which fits above 4 K.

I. INTRODUCTION

The isostructural RRh_4B_4 (R denotes rare earth) series of compounds includes several magnetic superconductors.[1] The subjects of this paper are $SmRh_4B_4$, a "coexistent antiferromagnet" in which the development of antiferromagnetic order below 0.87 K does not destroy the superconducting state that sets in below 2.7 K, and $ErRh_4B_4$, a "reentrant ferromagnet" that is superconducting at temperatures between 0.9 and 8.7 K (polycrystalline samples) but is a resistive ferromagnet below 0.9 K. The discovery of such materials, in which superconducting order and long-range magnetic order both occur, when they had formerly seemed incompatible, have provided new challenges to theorists to explain the phenomena observed and subsequent challenges to experimentalists to detect the subtle effects that will discriminate between the various theoretical treatments that have appeared.

Qualitatively, the myth of the incompatibility of superconductivity and magnetic order sprang from the observation that all superconducting states known to occur at the time involved the conduction electrons in a spin-paired diamagnetic state, while magnetic ordering above ~ 1 K (below which mere dipolar coupling of large moments can in principle cause magnetic order) requires polarization of the conduction electrons. For most of the famous magnetic superconductor materials, it appears to be complicated band structure (due to complicated crystal structure) that allows both superconductivity and magnetism to occur. In the RRh_4B_4 phases, superconductivity is attributed to rhodium d electron bands, which band-structure calculations[2] indicate have very low density at the rare-earth site, while magnetic ordering is attributed to the Ruderman-Kittel-Kasuya-Yosida (RKKY) interaction,[3] communicated apparently by rare-earth d electrons (although these are believed to overlap somewhat with the rhodium d electrons). In addition, RKKY ordering of localized rare-earth moments involves much less conduction-electron polarization than transition-metal magnetic ordering. With such a separation of functions, coexistent antiferromagnetism is possible, but simple long-range ferromagnetism cannot coexist—even in principle—with (s wave) superconductivity, because nonzero bulk magnetization is still incompatible with the Meissner effect (coexistence of very weak, "nearly" ferromagnetic, or spontaneous vortex-lattice states has been suggested). The two ordering interactions cannot be totally isolated from each other, however, and their interaction with each other can lead to effects not seen for either ordering in isolation.

Effects of the superconducting interaction on magnetic properties have proven difficult to find in the laboratory, other than the suppression of magnetic ordering temperatures by the onset of superconductivity in pseudoternary alloys.[4] Instead, most of the magnetic properties of the RRh_4B_4 materials have been found to be dominated by crystalline electric field (CEF) effects.[5] The muon spin relaxation (μSR) experiments reported here were undertaken to try to detect effects of "competition" between the superconducting and magnetic ordering interactions in the magnetic moment dynamics near the various ordering temperatures. Prior evidence of interesting spin dynamical effects has been found in ^{11}B NMR measurements of dilute alloys of heavy rare earths in YRh_4B_4,[6] but at such dilutions that no magnetic ordering occurs. Other researchers have reported on μSR in the (Ho,Lu)Rh_4B_4 system,[7] which we will discuss briefly below.

This paper discusses data on μSR in $SmRh_4B_4$ and $ErRh_4B_4$ (with YRh_4B_4 as a nonmagnetic analogue) obtained at TRIUMF. Preliminary results on low-temperature μSR in $SmRh_4B_4$ and some analysis of μSR in $ErRh_4B_4$ were reported elsewhere.[8,9] Here we report data on $SmRh_4B_4$ up to room temperature, and develop a consistent interpretation of the data in the two materials. After describing how the data were obtained in Sec. II (Experiment), we present the new data on $SmRh_4B_4$ and develop a "double relaxation" model to produce physically reasonable fits to the data in Sec. III (Results). To relate $SmRh_4B_4$ μSR to $ErRh_4B_4$ μSR and to begin to untangle the magnitude of the local field from its fluctuation rate, we present Sec. IV [Modeling the Muon Site(s)]. We then show that the deduced rare-earth fluctuation rates are understandable in terms of well-known paramagnetic mechanisms, except below 4 K in $SmRh_4B_4$, in Sec. V (Modeling The Rare-Earth Fluctuation Rate). Finally, in Sec. VI (Conclusions) we propose that the excess muon spin relaxation below 4 K in $SmRh_4B_4$ is associated with the magnetic ordering transition.

II. EXPERIMENT

Polycrystalline ingots of YRh_4B_4, $SmRh_4B_4$, and $ErRh_4B_4$ were prepared by arc melting and annealing in a manner typical for these materials.[1] The nonmagnetic superconductor YRh_4B_4 was included in the μSR study as a "control" material containing no electronic moments (but including ^{11}B nuclear moments). Powder x-ray diffraction indicated that the YRh_4B_4 sample contained approximately 13% (by volume) RhB and 6% of an unidentified phase, the $SmRh_4B_4$ sample about 15% RhB, 7% $SmRh_3B_2$ and perhaps a trace of elemental Sm, and the $ErRh_4B_4$ sample RhB and an unidentified phase to a total of about 5% of the volume. Superconducting transition temperatures (midpoint, ac susceptibility of a powdered portion) were 10.8 K for YRh_4B_4, 2.6 K for $SmRh_4B_4$ and 8.6 K for $ErRh_4B_4$.

The zero-field (ZF) μSR technique has been described in Ref. 10. Data reported here were obtained at TRIUMF's M20 "surface muon" beamline, with the apparatus described in Ref. 11. The cryostat was a Janis ^4He gas-flow type; for temperatures below 1.5 K, a custom ^3He evaporation stage was inserted down the central access. Trim coils allowed cancellation of the magnetic field at the sample to ± 0.1 G. Data (time histograms) were collected for opposing pairs of counter telescopes. In zero field, nontrivial data are provided by "backward" (B) and "forward" (F) histograms, whose theoretical (fitted) forms are

$$N_{B,F}(t)=b_{B,F}+N_0^{B,F}\exp(-t/\tau_\mu) \times[1\pm A_0^{B,F}G_{zz}(t)] , \quad (1)$$

where $t=0$ is the time that the polarized muon stops, $N_{B,F}(t)$ is measured in positron counts per unit time bin, $b_{B,F}$ is the time-independent random background, $N_0^{B,F}$ is a normalization factor (counts per bin at $t=0$ for the isotropic component), τ_μ is the muon lifetime, $A_0^{B,F}$ is the initial magnitude of the anisotropy or "asymmetry" of the parity-violating decay of the muon detected by the corresponding counter telescope ($+A_0^B$ corresponds to N_0^B and $-A_0^F$ to N_0^F) and $G_{zz}(t)$ is the muon spin-relaxation function—i.e., the correlation function

$$G_{zz}(t)\equiv 4\langle S_z^\mu(0)S_z^\mu(t)\rangle .$$

It is $G_{zz}(t)$ that contains information about the magnetic properties of the material in which the muons have stopped, because magnetic interactions cause the muon spin to evolve in time. The time-independent background can be measured (at TRIUMF, this is done by recording the counts for several tenths of a microsecond before $t=0$, achieved by the judicious placement of delay in the recording electronics) and subtracted to form $B(t)\equiv N_B(t)-b_B$ and $F(t)\equiv N_F(t)-b_F$. An "asymmetry histogram" can then be constructed from data for opposing counters by taking the difference divided by the sum:

$$A(t)\equiv\frac{B(t)-F(t)}{B(t)+F(t)} . \quad (2)$$

For *identical* counters [defined by $N_0^B=N_0^F=N_0$ and $A_0^B=A_0^F=A_0$], the corresponding theoretical form would be just $A(t)=A_0G_{zz}(t)$. In general, however, opposing counters cannot be made identical and the instrumental parameters $\alpha\equiv N_0^F/N_0^B$ and $\beta\equiv A_0^F/A_0^B$ must be included in the fitting procedure. The experimental asymmetry $A(t)$ is then modelled rigorously by

$$A(t)=\frac{(1-\alpha)+(1+\alpha\beta)A_0^BG_{zz}(t)}{(1+\alpha)+(1-\alpha\beta)A_0^BG_{zz}(t)} , \quad (3a)$$

which is the function actually used in fitting asymmetry spectra. For display, this relationship is inverted to yield the "corrected asymmetry" in terms of the instrumental asymmetry and the fitted empirical parameters:

$$A_0^BG_{zz}(t)=\frac{(\alpha-1)+(\alpha+1)A(t)}{(\alpha\beta+1)+(\alpha\beta-1)A(t)} . \quad (3b)$$

Removal of backgrounds and reduction of two "raw" time histograms to one asymmetry spectrum reduces the computer time required to fit the data. Moreover, while the "normalization ratio" α is rarely very close to unity and is always subject to systematic variations (e.g., due to an intermittent discriminator), the "asymmetry ratio"

$\beta \approx 1$ is usually quite stable and the approximation $\beta \cong 1$ ($A_0^F \cong A_0^B \cong A_0$) is routinely used. The corresponding simplification of Eq. (3a) reduces the number of fitted parameters still further. When the time-independent backgrounds are not well known, however, they must be fitted and Eq. (2) cannot be used. In this case the $N_B(t)$ and $N_F(t)$ histograms can be fitted separately but simultaneously, using all the empirical parameters for both B and F with a common $G_{zz}(t)$.

III. RESULTS

Figure 1 shows ZF μSR asymmetry spectra in YRh_4B_4 at (a) room temperature and (b) 220±5 K. Spectra taken at temperatures below 220 K, including those in the superconducting state, were indistinguishable from that shown in Fig. 1(b), a typical example of the well-known[10] "static Gaussian Kubo-Toyabe" shape due to stationary muons sampling a random, but static, Gaussian distribution of local magnetic fields:

$$g_{zz}^{\mathrm{KT}}(t)=\tfrac{1}{3}+\tfrac{2}{3}(1-\Delta_{\mu B}^2 t^2)\exp\left[-\frac{\Delta_{\mu B}^2 t^2}{2}\right], \quad (4)$$

where $\Delta_{\mu B}/\gamma_\mu$ is the (single-component) rms width of the distribution of probabilities of local magnetic fields (γ_μ is the muon gyromagnetic ratio, so Δ has the units of a muon precession rate). The subscript μB denotes the distribution of local fields at the muon *due to* the boron moments; more complicated situations will be described below in a similar notation. The fitted value of $\Delta_{\mu B}$ in YRh_4B_4 corresponds to an rms width of 4.0±0.2 G in the distribution of each component of the local field at the μ^+, consistent with dipolar coupling to the ^{11}B nuclear moments in the sample. The spectrum at room temperature is consistent with *hopping* of the muons between sites at a rate ν_h. The conventional notation for the *dynamic* Kubo-Toyabe relaxation function including the effect of hopping (using a "strong collision"[12] model) is $G_{zz}^{\mathrm{KT}}(\Delta,\nu_h,t)$; it is obtained from the *static* Kubo-Toyabe function $g_{zz}^{\mathrm{KT}}(\Delta,t)$ by numerical integration of the Volterra integral equation describing the strong-collision model,[13]

$$G_{zz}^{\mathrm{KT}}(\Delta,\nu_h,t)=e^{-\nu_h t}g_{zz}^{\mathrm{KT}}(\Delta,t) + \nu_h\int_0^t dt' G_{zz}^{\mathrm{KT}}[\Delta,\nu_h,(t-t')] \times e^{-\nu_h(t-t')}g_{zz}^{\mathrm{KT}}(\Delta,t') . \quad (5)$$

The line shown in Fig. 1 is the result of fitting G_{zz}^{KT} to the data, assuming the field distribution found at low temperatures. The deduced μ^+ hop rate at room temperature in YRh_4B_4 is $\nu_h = 1.6\pm0.2\ \mu s^{-1}$, which is rather slow, but not unusual for muons in a complicated lattice.[10]

Figure 2 shows ZF μSR spectra in $SmRh_4B_4$ at room temperature and 200±10 K. Spectra taken at 230±15 K and 275±15 K had shapes intermediate between these. The spectrum at 200 K is identical to those in YRh_4B_4 for $T \lesssim 220$ K, indicating a stationary muon coupled to static ^{11}B nuclear moments, but not to the much larger trivalent samarium electronic moments. The spectra above 200 K could again be fitted assuming muon hopping within the same field distribution as for YRh_4B_4. Deduced hop rates are $\nu_h = 0.06\pm0.02\ \mu s^{-1}$ at 230 K, $\nu_h = 0.11\pm0.02\ \mu s^{-1}$ at 275 K, and $\nu_h = 0.42\pm0.04\ \mu s^{-1}$ at room temperature (even slower than in YRh_4B_4).

Spectra of $SmRh_4B_4$ below 200 K begin to differ from those of YRh_4B_4. Qualitatively, below 200 K the recovery of the asymmetry at late times becomes weaker again, indicating that the local field seen by a given muon

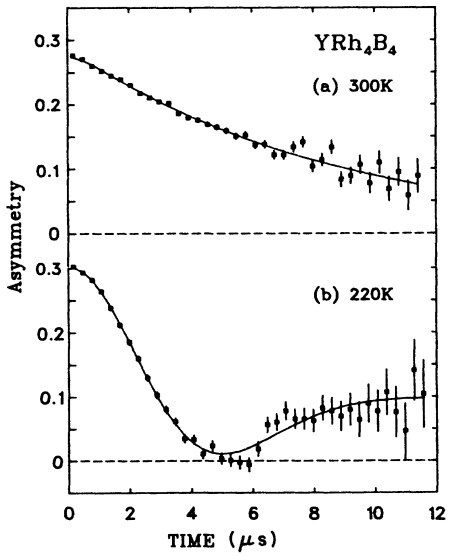

FIG. 1. ZF μSR asymmetry spectra of YRh_4B_4 at (a) room temperature and (b) 220±5 K. Solid lines are least-squares fits discussed in the text. Initial asymmetries differ because the two spectra were taken in different sample holders at different times.

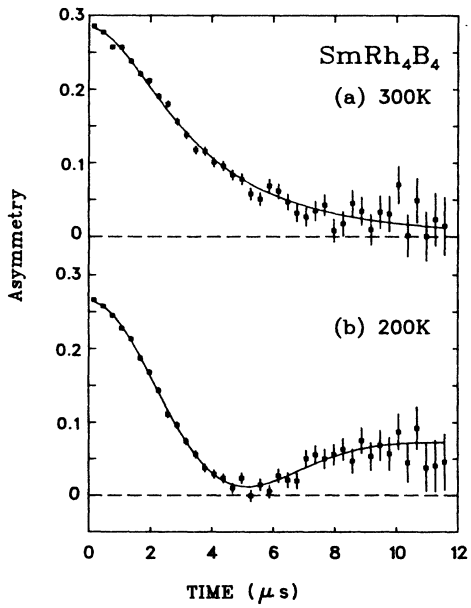

FIG. 2. ZF μSR asymmetry spectra of $SmRh_4B_4$ at (a) room temperature and (b) 200 K. Solid lines are least-squares fits discussed in the text.

is not truly static. It is unlikely, however, that this is the result of muons starting to hop again below 200 K. More probably it is the local field itself that has begun to fluctuate. This hypothesis is borne out by a more detailed examination of the data, below. For $T \leq 80$ K, the decay of asymmetry in the early bins becomes *faster* than in the spectrum at 200 K, which means that the rms local field must be greater below 80 K than at 200 K. In Fig. 3 we illustrate this by overlaying ZF-μSR spectra in $SmRh_4B_4$ at 200 and 25 K. Below 80 K, no recovery of asymmetry is seen at late times, but only below 10 K are spectra well fitted by a simple exponential relaxation of the asymmetry. The only physically reasonable interpretation of these results is that the samarium atomic moments generate a much larger instantaneous field at each muon than the ^{11}B nuclei, but that above 200 K the Sm^{3+} moments are fluctuating so rapidly that they are completely decoupled from the muon spin. Then, as the temperature is reduced below 200 K, the fluctuation rate of the Sm^{3+} moments becomes sufficiently slow to begin coupling to the other moments in the material.

The simplest version of this picture is a static field distribution (due to ^{11}B nuclei) persisting at all temperatures, to which is added a rapidly fluctuating field distribution due to Sm atomic moments. It is straightforward to show that when a static field distribution and a rapidly fluctuating field distribution (rapidly meaning $\nu_{Sm} \gg \Delta_{\mu Sm}$, where ν_{Sm} is the average fluctuation rate of the field and $\Delta_{\mu Sm}/\gamma_\mu$ is its component rms width) affect the muon in a statistically independent fashion, the resulting relaxation function is the product of the relaxation functions due to each of the two distributions acting alone.[14] Assuming, as is usually done, that the field distribution at the muon due to the samarium ionic moments is approximately Gaussian, and that its fluctuations can be approximated by a strong-collision model (the surprisingly wide range of circumstances under which these are good approximations is discussed below), the fast-fluctuation limit of the relaxation function due to samarium moments alone is an exponential decay:

$$G_{zz}^{\mu Sm}(\Delta_{\mu Sm}, \nu_{Sm}, t) \rightarrow \exp\left[-\frac{2\Delta_{\mu Sm}^2 t}{\nu_{Sm}}\right] . \quad (6)$$

The product relaxation function is then predicted to be the static Gaussian Kubo-Toyabe seen at 200 K multiplied by an exponential, with the decay rate of the exponential a function of temperature:

$$G_{zz}^{tot}(t) = \left[\tfrac{1}{3} + \tfrac{2}{3}(1-\Delta_{\mu B}^2 t^2)\exp\left[-\frac{\Delta_{\mu B}^2 t^2}{2}\right]\right] \times \exp\left[-\frac{2\Delta_{\mu Sm}^2 t}{\nu_{Sm}}\right] . \quad (7)$$

It is important to note, however, that Eq. (7) implies that each asymmetry spectrum at a temperature below 200 K should fall strictly below the asymmetry spectrum at 200 K for all times $t > 0$. This requirement is clearly not satisfied by the data, as shown in Fig. 3.

The failure of the simple model above suggests that a more complicated model is necessary. As temperature decreases below 200 K and the samarium ionic moments begin to couple to the muon, they must (at some temperature) also begin to couple to the ^{11}B nuclear moments, so that the ^{11}B moments (and the field they generate at the muon) no longer remain static on a 10 μs timescale (however, this is somewhat at variance with results of ^{11}B NMR in $SmRh_4B_4$, where T_1 was observed to be milliseconds or longer in applied fields[15,16]). Figure 4 illustrates the interactions of the three types of moments. A similar process for muons in MnSi has been called[17] "muon-nuclear spin double relaxation." Considering the samarium-boron coupling and the boron-generated field at the muon in the semiclassical manner of the Kubo-

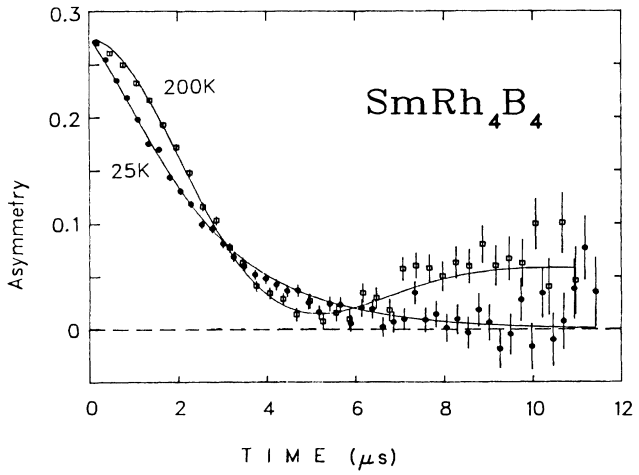

FIG. 3. ZF μSR asymmetry spectra of $SmRh_4B_4$ at 200 K (open squares) and 25 K (solid circles), overlaid. Solid lines are the result of a simultaneous fit of the spectra to the double-relaxation model described in the text.

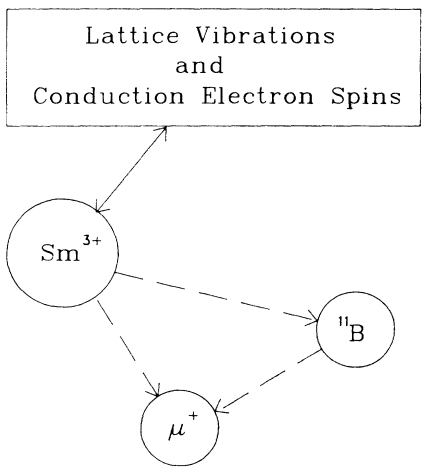

FIG. 4. The three types of magnetic moment in $SmRh_4B_4$ and their couplings in the double-relaxation model in the text. Dashed arrows indicate dipole coupling, the solid arrow indicates the interactions discussed in Sec. V.

Toyabe calculation, and with some assumptions to simplify the calculation, the boron-generated field at the muon obeys

$$\frac{\langle H(0)\cdot H(t)\rangle}{\langle H^2(0)\rangle}\approx\exp\left[-\frac{2\Delta_{B\mathrm{Sm}}^2 t}{\nu_{\mathrm{Sm}}}\right] \tag{8}$$

where $\Delta_{B\mathrm{Sm}}$ is the rms field component at the boron nucleus due to samarium moments (times the magnetogyric ratio γ_B for ^{11}B). Such a decay in field self-correlation can be reproduced by the strong-collision model mentioned previously (in fact, the process would be better represented as Gaussian-Markovian, but the difference between the dynamic relaxation functions generated by the two versions is small,[18] and the strong-collision calculation was available in our fitting program). Thus we can replace the static Kubo-Toyabe term in the product relaxation function by the dynamic Kubo-Toyabe, to represent the action of the boron-generated field on the muon:

$$G_{zz}^{\mathrm{tot}}(t)=G_{zz}^{\mathrm{KT}}(\Delta_{\mu B},\nu_B^{\mathrm{eff}},t)\exp\left[-\frac{2\Delta_{\mu\mathrm{Sm}}^2 t}{\nu_{\mathrm{Sm}}}\right], \tag{9}$$

where

$$\nu_B^{\mathrm{eff}}=\frac{2\Delta_{B\mathrm{Sm}}^2}{\nu_{\mathrm{Sm}}}. \tag{10}$$

The three different Δ parameters should be constant or weak functions of temperature (due to CEF effects). They have been assumed independent of temperature in fitting. Examples of fits to the data are shown in Fig. 3.

While the magnitude of $\Delta_{\mu B}$ is fixed by the spectra near 200 K, the assumption of the fast fluctuation limit for the samarium field at both the boron nuclei and the muon implies that only a lower bound can be placed on $\Delta_{B\mathrm{Sm}}$, $\Delta_{\mu\mathrm{Sm}}$, and ν_{Sm}. Beyond that, these three can be scaled up together, keeping the proportionality $\Delta_{B\mathrm{Sm}}^2:\Delta_{\mu\mathrm{Sm}}^2:\nu_{\mathrm{Sm}}$ constant (at fixed temperature). This double relaxation model fits the $SmRh_4B_4$ data fairly well from 200 K down to below 10 K, where, as mentioned before, it is sufficient to assume simple exponential muon spin relaxation. $G_{zz}^{\mathrm{tot}}(t)$ becomes a simple exponential when the "hop rate" ν_B^{eff} [Eq. (10)] becomes much larger than $\Delta_{\mu B}$:

$$G_{zz}^{\mathrm{tot}}(t)\rightarrow\exp\left[-\left[\frac{2\Delta_{\mu\mathrm{Sm}}^2}{\nu_{\mathrm{Sm}}}+\frac{\Delta_{\mu B}^2\nu_{\mathrm{Sm}}}{\Delta_{B\mathrm{Sm}}^2}\right]t\right]. \tag{11}$$

Fits over the 10–200 K temperature range imply a ratio of about 5.5 between the rms field at the ^{11}B nucleus and that at the muon, with lower bounds of about 330 and 60 G, respectively; the large value of this ratio in circumstances where both spins should be primarily dipole coupled is surprising (as will be seen in more detail below). The value of the field at the boron nucleus may have been inflated somewhat by the replacement of the (continuous) random-walking boron field at the muon by the (discontinuous) jumping field (with the same correlation time) of the strong-collision dynamic Kubo-Toyabe function. If conduction electrons contribute substantially to the coupling of rare-earth moments to ^{11}B nuclei (RKKY mechanism), the effective field deduced from our dipole-coupling assumption would also be increased. The corresponding lower bound values (for $\Delta_{\mu\mathrm{Sm}}/\gamma_\mu=60$ G) of the samarium fluctuation rate as a function of temperature are shown in Fig. 5.

Below 10 K, simple exponential spin relaxation was fitted to the data, as reported previously.[8] It is possible to continue to use the double-relaxation model in its exponential limit form [Eq. (11)] to interpret this. One reason to do so is that at 10 K the derived parameters mean that one third of the exponential relaxation rate is still due to the boron nuclear moments (they have not yet become insignificant, as the samarium moments are still partially decoupled by their fluctuations). The samarium-field fluctuation rate extracted below 10 K (for $\Delta_{\mu\mathrm{Sm}}/\gamma_\mu=60$ G) is shown as a function of temperature in Fig. 6.

There is no discernible effect on the μSR spectra in going through the superconducting transition at 2.6 K. As temperature decreases to within a few tenths of a kelvin of the magnetic transition temperature, however, some qualitative changes occur. The initial asymmetry, which is constant from room temperature down to about 2 K, decreases somewhat and the fit χ^2 for simple exponential relaxation becomes somewhat poorer. The reduction of the observed initial asymmetry below 2 K might be due to superfluid helium creeping onto the cryostat window or the surface of the sample (as has been seen in other experiments with this cryostat), or to muons stopping in a nonmagnetic environment (so that the spins do not relax, contributing instead a shift in the apparent zero-asymmetry baseline). No straightforward elaboration of the relaxation function improved the fits significantly. Below the magnetic transition (0.87 K) no ordered state precession was seen,[8] but rather a sum of two exponentials relaxing from nearly full asymmetry. Thus the field distribution, while different, still appears random to the sampling muons in the ordered state. We will discuss this low-temperature behavior further, below.

The $SmRh_4B_4$ μSR data just discussed do not resemble

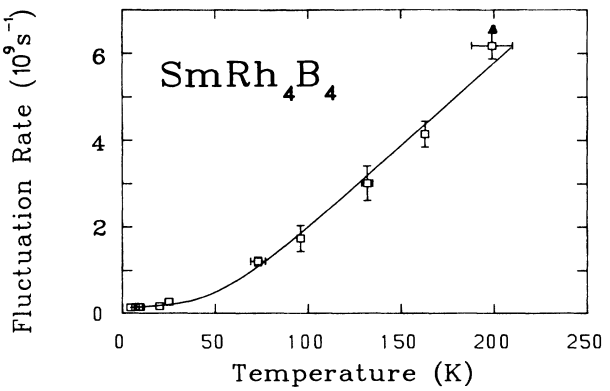

FIG. 5. The fluctuation rate of the field generated by the samariums in $SmRh_4B_4$ as deduced from fits of the double-relaxation model to the μSR data for $T>4$ K. The solid line is the fit of the paramagnetic mechanisms model discussed in Sec. V.

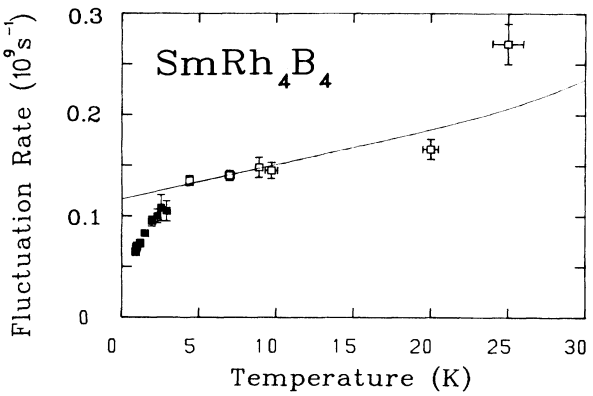

FIG. 6. The fluctuation rate of the field generated by the samariums in $SmRh_4B_4$ by extension of the double-relaxation model down to the magnetic ordering temperature (0.87 K). The solid line is the extension of the paramagnetic model line of Fig. 5.

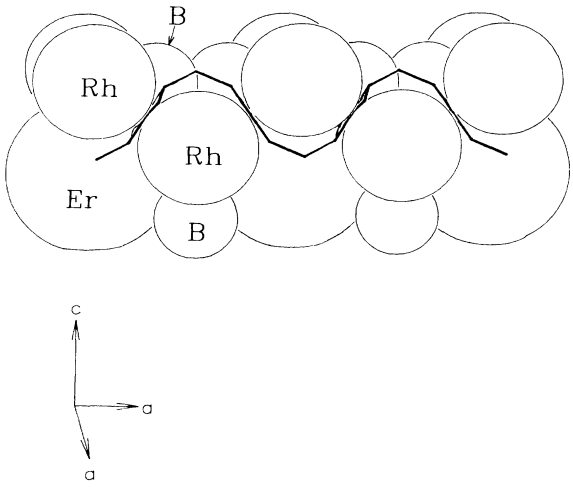

FIG. 7. Schematic drawing of the basal-plane channel structure of possible muon sites in the RRh_4B_4 structure.

the $ErRh_4B_4$ μSR data presented in Ref. 9. There, the muon asymmetry relaxed to zero rapidly even at room temperature and it was found necessary to use the sum of two exponentials to fit the relaxation well. Below 50 K, the relaxation time of the faster part of the signal becomes shorter than our apparatus dead time (≈ 10 ns). The relaxation is much faster than in $SmRh_4B_4$ because of the much larger erbium magnetic moment. The two-exponential relaxation was interpreted as being due to two different muon sites in $ErRh_4B_4$ with quite different rms fields, while only one site is necessary in the fitting of $SmRh_4B_4$ data above. We were unable to invent a two-site model for the $SmRh_4B_4$ data that was not more complicated than the (single muon site) double-relaxation model above. After fitting, however, the extracted rare-earth-field fluctuation rates as functions of temperature are qualitatively similar for the two materials above about 7 K (and the loss of signal in $ErRh_4B_4$ below 50 K results in no information for it at all below 7 K).

IV. MODELING THE MUON SITE(S)

One major uncertainty in interpreting the μSR data above is the location of the stopped muons in the lattice. The crystal structure is complicated and the muons cannot be expected to sit at positions of high symmetry. Using the tabulated, "usual" covalent radii of the ions involved, the most room is available between the rare earths and the rhodium-boride clusters, while the higher symmetry site in the centre of the RhB cluster is considerably smaller. A number of slightly different sites are available next to the rare earth ions, all with similar volumes, and probably close enough together to form a channel structure in the plane perpendicular to the c axis of the tetragonal structure (Fig. 7). This suggests that the muon diffusion seen above about 200 K will be preferentially in this basal plane. The site at the centre of the RhB cluster is, on the other hand, isolated. A muon diffusing from one such RhB center to the next must cross the channel structure of the other set of sites in doing so.

We have modeled the (paramagnetic state) magnetic field distributions at these sites by Monte Carlo simulation, assuming dipole coupling. For each site, a cluster of roughly 400 of the magnetic ions (borons for evaluation of the YRh_4B_4 and high-temperature $SmRh_4B_4$ cases, rare earths for the rapid-relaxation cases) in a sphere surrounding the site was generated by a program based on ORTEP (Oak Ridge Thermal Ellipsoid Plotter) routines. For each Monte Carlo iteration magnetic moment orientations were then assigned randomly and the dipole field at the centre was evaluated. Isotropic moments were used, to keep the calculation simple. Because we measured polycrystalline samples, the Monte Carlo program also chose random orientations of the crystal axes with respect to the "observer" (the initial muon spin direction).

The rms fields found by simulation at various positions in the crystal structure are summarized in Table I. All of the boron-field distributions mentioned in the table were fairly well approximated by Gaussians with widths indicated in the table, as were those erbium-field distributions with rms values less than 7000 G. The erbium-field distributions with rms values above 7500 G were distinctly

TABLE I. Monte Carlo polycrystalline average rms component dipole magnetic fields at various positions in the $ErRh_4B_4$ structure. The first four positions are on the channel structure between the rare-earth ions and the RhB clusters, (0,0,0) is the center of the RhB cluster and (0,0.325,0.847) is the position of boron itself (where the rare-earth-generated field distribution is of interest for the double relaxation model).

Unit-cell coordinates	^{11}B field (G)	Er field (G)
(0.50,0.100,0.05)	5.7	7400
(0.50,0.175,0.15)	5.7	8400
(0.30,0.300,0.20)	3.0	7800
(0.25,0.250,0.25)	3.5	5600
(0,0,0)	2.2	3400
(0,0.325,0.847)		3400

"flat-topped," however (see Fig. 8). In a separate publication,[19] the distorting effect of such flat-topping on the standard Gaussian Kubo-Toyabe relaxation function has been shown to be surprisingly small. The samarium-generated field distributions at these sites in $SmRh_4B_4$ should be obtained by rescaling the erbium-generated distributions by the ratio of the free-ion moments ($0.72\mu_B$ for Sm versus $9.0\mu_B$ for Er) times a number near unity representing the difference in unit cell sizes.

The Monte Carlo rms component ^{11}B field at the site in the center of the RhB cluster is considerably less than the value of 4.0 G observed in YRh_4B_4 and $SmRh_4B_4$, while the channel sites's boron rms values span a range covering the observed value, although none of the four sites chosen reproduce the value itself. This suggests that muons sit somewhere on the channel structure in those two materials. With regard to $ErRh_4B_4$, we nominate the RhB site as the low-field site and (somewhere on) the channel structure as the high-field site. The ratio of Monte Carlo rms fields at these two sites is 0.5 ± 0.1, in agreement with the ratio deduced from the fits to the $ErRh_4B_4$ data (0.38 ± 0.07) in Ref. 9. Table I also shows that the rms dipole samarium field at the boron is predicted to be about one half the rms dipole field at the muon in $SmRh_4B_4$, contrary to dipolar field widths deduced from fitting the double-relaxation model to the μSR data, as was mentioned above.

Other than this difficulty in handling the samariums acting through the boron nuclei on the muon, the numerical modelling of candidate site field distributions is reasonably consistent with the observations in these materials. High- and low-field sites are available, but it is not clear why both should be seen in $ErRh_4B_4$ and only one seen in $SmRh_4B_4$ (although their lattice parameters do differ[1]). The rms rare-earth-generated dipole fields at these sites are above the lower bounds derived from the fits to the data, so that the fast-fluctuation limit is consistent for those fits. The modeling has been of the strictly paramagnetic state and will not apply in magnetically ordered states, nor in any critical regimes at temperatures just above those orderings.

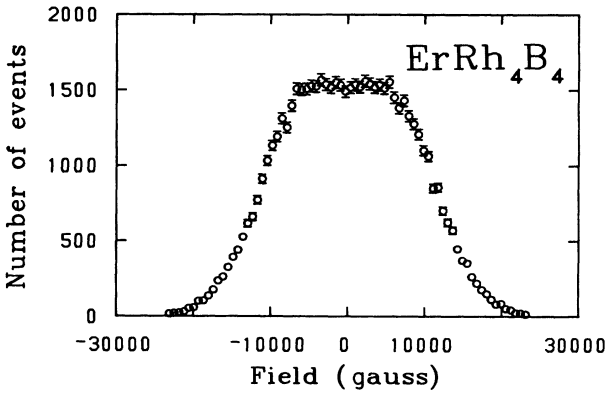

FIG. 8. Monte Carlo polycrystalline average (component) dipole field distribution at the largest interstitial (candidate muon) site in $ErRh_4B_4$.

V. MODELING THE RARE-EARTH FLUCTUATION RATE

In the paramagnetic state, well above any ordering temperature, rare-earth spin fluctuations in a metal can be caused by the "spin-lattice interaction," by Korringa scattering of conduction electrons and/or by any paramagnetic remnants of the RKKY and dipolar interactions that cause the low-temperature ordering.

The spin-lattice interaction is reviewed in Ref. 20. Lattice vibrations (phonons) mix the (static-limit) CEF spin substates of each rare-earth ion, causing transitions between them. Given two CEF levels $|a\rangle$, and $|b\rangle$ at energy (ϵ_{ab}) less than $k_B\Theta_D$ (Θ_D is the Debye temperature) above it, real-phonon transitions dominate, resulting in an average fluctuation rate ν_{ab} from $|a\rangle$ to $|b\rangle$ given by

$$\nu_{ab}=\frac{C\epsilon_{ab}^3\,|\langle a|V_{\rm ph}|b\rangle|^2 P(a)}{\exp(\epsilon_{ab}/k_BT)-1}\ , \tag{12}$$

where

$$C=\frac{3}{2\pi\rho\hbar^4 v^5}\ , \tag{13}$$

$\langle a|V_{\rm ph}|b\rangle$ is the (phonon) dynamic CEF coupling between $|a\rangle$ and $|b\rangle$, $P(a)$ is the probability that the system is in the state $|a\rangle$ initially, ρ is the density of the material, and v is the Debye model (isotropic, frequency independent) speed of sound in the material. Virtual phonon processes will not be considered here: most (perhaps all) CEF levels lie below the Debye energy ($k_B\Theta_D$) in these rhodium borides (the highest CEF state in $SmRh_4B_4$ is at about 200 K, in $ErRh_4B_4$ about 120 K),[5] and in such circumstances virtual phonon rates are orders of magnitude smaller than the above. The dynamic CEF couplings are difficult to measure or estimate in detail. In Ref. 20 it is argued that

$$|\langle a|V_{\rm ph}|b\rangle|^2\approx\epsilon_{ab}^2\ . \tag{14}$$

[Reference 21 has argued, on the basis of a point-charge calculation, that for each order n of the multipole expansion of the CEF coupling there should be an additional multiplicative factor of $(n+1)^2$. In these materials the CEF effects are dominated by the electric field gradient $n=2$; so if the point-charge argument remains valid for such metals, estimates of C from Eq. (13) and $\nu_{\rm SL}$ from Eq. (15) below will be increased by about an order of magnitude.] The complete set of CEF energy levels (E_i) in $ErRh_4B_4$ has been estimated,[5] and the associated levels for $SmRh_4B_4$ can be derived from them (effects of coupling to states of higher total angular momentum J appear to be necessary for samarium to reproduce recent data on the anisotropy of single crystals of $SmRh_4B_4$,[22] but these effects are only now being resolved[23]). The spin-lattice transition rate $\nu_{\rm SL}$ is then the sum of the rates between all pairs of CEF levels,

$$\nu_{\rm SL}=2C\sum_i P(i)\sum_{E_j>E_i}\left[\frac{(E_j-E_i)^5}{\exp[(E_j-E_i)/k_BT]-1}\right]\ , \tag{15}$$

where the probability of occupation is governed by the

Boltzmann distribution over the CEF levels, and the leading factor of 2 compensates for the exclusion of "downward" transitions ($E_j < E_i$) in the sum—in equilibrium, the rates of such transitions must equal those of the corresponding "upward" transitions. Note that Eq. (15) describes an equilibrium fluctuation rate, not a relaxation rate. Relaxation rates can be derived from Eq. (15) using the argument that for small displacements from equilibrium the rate of relaxation back to equilibrium is governed by the equilibrium fluctuation rate.[24] For muons in magnetic materials, the standard assumption (used in this paper) is that the ion-spin system remains in equilibrium. The value of C is not well known because the (Debye model) speed of sound is not well known for these materials. The speed of sound found in a polycrystalline sample of $ErRh_4B_4$ in a measurement[25] of ultrasonic attenuation was 5.0×10^7 cm/s. Assuming this value and densities of about 10 g/cm^3, C is of order 0.06 $K^{-5}s^{-1}$. We have evaluated ν_{SL} numerically, using that value for C. For $SmRh_4B_4$ the rate is very small below 10 K, rises to $\approx1\times10^6$ s^{-1} at 20 K, reaches $\approx1\times10^7$ s^{-1} at 27 K and becomes nearly linear in temperature above 80 K, rising to about 1×10^{10} s^{-1} at 200 K.

The Korringa and paramagnetic limit fluctuation rates in $SmRh_4B_4$ were estimated in Ref. 15. Assuming the $s-f$ exchange Korringa scattering expression,[26]

$$\nu_{\mathrm{Korr}}=\pi[\mathscr{J}N(0)]^2k_BT/\hbar\ , \tag{16}$$

where $\mathscr{J}$ is the $s-f$ exchange constant and $N(0)$ is the density of states at the Fermi level, and using reasonable estimates for those two quantities, Ref. 15 found $\nu_{\mathrm{Korr}}\approx[2.4\times10^6\ \mathrm{K^{-1}s^{-1}}]T$. For the paramagnetic limit of the RKKY interaction, Ref. 15 quotes an expression derived for dilute magnetic impurities in a host:[27]

$$\nu_{\mathrm{RKKY}}=\left[\frac{S(S+1)}{6}\right]^{1/2}\frac{N(0)\mathscr{J}^2c}{9\hbar}\ , \tag{17}$$

where S is the total spin and c is the concentration, which should be less than 0.1 for the expression to be accurate. There is apparently no analytic expression for $c\approx1$, but Ref. 15 estimates $\nu_{\mathrm{RKKY}}\approx3.6\times10^7$ s^{-1} for $SmRh_4B_4$.

The low magnetic ordering temperatures of the RRh_4B_4 compounds mean that the dipole interaction may compete with the RKKY interaction in establishing the ordered state. If so, then the dipole interaction may also be competitive with RKKY in causing paramagnetic fluctuations.

The estimates above suggest that once the temperature is above the critical regime (if any) near the magnetic ordering, the paramagnetic RKKY mechanism should dominate the fluctuations below about 10 K in $SmRh_4B_4$, the Korringa mechanism should contribute to temperature dependence from about 10 to 30 K and the spin-lattice fluctuations should take over above that. We wish now to relate these rare-earth single-ion fluctuation rates to the (strong-collision model) effective fluctuation rate of the field at the muon. The field at the muon is the sum of contributions from a number of ions, and if only one of those ionic moments changes (even if in a manner consistent with the strong collision model), the field at the muon after the change retains some memory of its value before the change, in violation of the simple strong-collision model. In general, it is then more correct to use the term "correlation time," the inverse of the "fluctuation rate," but in these circumstances, the effect of the memory retention across a single-ion fluctuation on the apparent fluctuation rate at the muon is simply to multiply the single-ion fluctuation rate by a positive number less than one (the two rates are proportional).

We have least-squares fitted the sum of the three mechanisms to the $SmRh_4B_4$ fluctuation rate above 4 K, with the overall magnitude of each of the three adjustable by the fitting routine. The fit (solid line in Figs. 5 and 6) returns an RKKY rate of $\nu_{\mathrm{RKKY}}\approx1.2\times10^8$ s^{-1}, a Korringa rate constant of $\nu_{\mathrm{Korr}}/T=(3.4\pm0.6)\times10^6$ $K^{-1}s^{-1}$ and a spin-lattice constant of $C\approx0.02$ $K^{-5}s^{-1}$. These are within factors of 3 of the independent estimates above, which is acceptable given the crudeness of some of the approximations, but the apparent RKKY rate is high while the apparent spin-lattice rate is low. The sum of the three mechanisms was not fitted to the data below 4 K because it cannot reproduce the negative second derivative of rate with respect to temperature that is obvious in Fig. 6. The rapid decrease in the apparent fluctuation rate (i.e., the increase in the muon spin-relaxation rate) below 4 K is probably associated with the orderings at 2.7 and 0.87 K.

The same three paramagnetic fluctuation mechanisms should also govern the erbium fluctuations in $ErRh_4B_4$ well above the ordering temperatures. The formula for the Korringa rate [Eq. (16)] does not depend on the properties of the rare-earth ion (the exchange constant $\mathscr{J}$ is "per unit spin"), so that rate should be the same as in $SmRh_4B_4$. The RKKY rate [Eq. (17)] depends on $S(S+1)$, which in the rare earths is represented by the deGennes[28] factor $(g_J-1)^2J(J+1)$. The deGennes factor is smaller for trivalent erbium than for samarium and it enters as the square-root here, causing a reduction of the predicted RKKY rate by 25%, to $\nu_{\mathrm{RKKY}}(\mathrm{Er})=2.7\times10^7$ s^{-1}. The difference between the spin-lattice rates for the various ions lies in the distribution of the CEF levels in Eq. (15) and, for the CEF level scheme discussed above, causes a slower fluctuation rate in $ErRh_4B_4$ than in $SmRh_4B_4$, for a given value of C. Note that any dipole-coupling fluctuations should be much stronger in $ErRh_4B_4$, because the magnetic moment of trivalent erbium is much larger than that of samarium.

For the same sort of fit of these paramagnetic mechanisms to the erbium-field fluctuation rate reported in Ref. 9 from 7 to 155 K (Fig. 9), the observed rate versus temperature is not reproduced as well as for $SmRh_4B_4$. The apparent RKKY rate is 3×10^8 s^{-1}, an order of magnitude above the estimate; the Korringa rate constant is less than 4×10^5 $K^{-1}s^{-1}$ and consistent with zero; and the apparent spin-lattice rate C is 0.4 $K^{-5}s^{-1}$, also an order of magnitude larger than the prediction. The RKKY and the Korringa terms contribute below 50 K, where only a small remnant initial asymmetry was observed, so that systematic (baseline and background) effects were much harder to control and are not represented in the error bars on the graph. From 50–155 K, the $ErRh_4B_4$ and $SmRh_4B_4$ fluctuation rates are consistent if the samarium rates are scaled up to match. (Recall that the vertical

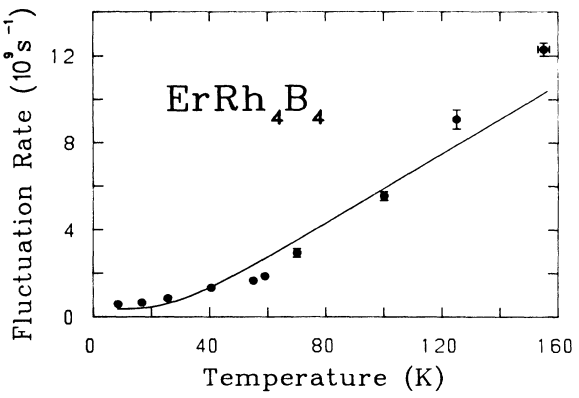

FIG. 9. The least-squares fit (solid line) of the paramagnetic mechanisms model to the fluctuation rate of the erbium-generated field in $ErRh_4B_4$ (data from Ref. 9) for $7 < T < 155$ K.

scales on Figs. 5, 6, and 9 are lower bounds: they can be multiplied by any number greater than one.) The "sidestep" in the upward trend of the (apparent) erbium-field fluctuation rate between 155 and 200 K (seen in Fig. 2 of Ref. 9) can be explained as due to the onset of muon hopping. The larger high-field site asymmetry in the data and the larger number of (high-field) channel-structure sites compared to the (low-field) RhB-cluster sites that seem available in the crystal structure suggest that when hopping starts, most muons that initially stop in a low-field site will make their first hop to a high-field site, but not vice versa. The function that was fitted to the data above 200 K did not allow for this possibility. Thus the onset of hopping will increase the "average" field that the muons see, causing faster depolarization to compensate the decoupling effect of faster field-fluctuation rate as temperature increases, in a narrow range. The argument ceases to apply as soon as the hop rate approaches the high-field site stationary-muon depolarization rate, but at that temperature the sites are being averaged over and two exponentials are no longer necessary to fit the data (as temperature approaches 300 K in $ErRh_4B_4$).

The μSR data on $SmRh_4B_4$ and $ErRh_4B_4$ discussed in this paper are generally consistent with μSR data on (Ho,Lu)Rh_4B_4 alloys published by other authors,[7] and the interpretation scheme above could quite likely be applied to those alloys too. In $HoRh_4B_4$, as in $ErRh_4B_4$, the muon spin relaxation becomes too rapid to resolve at low temperatures, for the same reason. Those authors attempt to deduce information about holmium moment dynamics from the low temperature, reduced amplitude signal, but the details at these temperatures are likely to be different in $HoRh_4B_4$ versus $ErRh_4B_4$, because the two rare-earth ions have quite different low-temperature CEF level configurations in these materials.[5] In a sample with only 2% Ho in $LuRh_4B_4$, as in $SmRh_4B_4$, the fluctuation rate of the holmium electronic moments becomes so fast above 50 K (in comparison to the rms field they produce at the muon, which is reduced by the dilution with lutetium) that they are decoupled from the muons, which then see only a static nuclear dipolar field distribution attributable to ^{11}B nuclei, followed by the onset of Ho-μ coupling as the temperature is lowered.

We are left with the apparent excess slowing down in $SmRh_4B_4$ below 4 K (Fig. 6). Since the muon spin relaxation is exponential in this range, it is pure slowing down only if the field distribution at the muon site retains the same form as at higher temperature. In general, distortion of the field distribution can occur as well as slowing down of spin fluctuations as short-range correlations set in. There is still no evidence of the superconducting transition (2.6 K) in the μSR data. Note that while Ref. 8 treated the relaxation as though it diverged at T_N, this may not have been an appropriate assumption. Unlike bulk susceptibility, which at certain types of transition can diverge in the sense that its value will be limited only by the size of the sample that is undergoing the transition, there are limits on spin-relaxation rates (the energy density of the effective field causing the relaxation must remain finite, for example, and it is difficult to imagine a circumstance that would relax muon polarization faster than about 4.5 GHz [the hyperfine coupling in muonium]). Thus the use of the term "divergence" for a relaxation rate (measured by μSR, NMR, or whatever) merely indicates that it increases until no longer measurable as the transition is approached (see, for example, Refs. 18 and 29). In $SmRh_4B_4$, however, the maximum paramagnetic relaxation rate observed is less than the rate just below T_N. As short-range correlations mimicking the ordered state set in, the rms components of the field at the muon should approach those in the ordered state just below the ordering temperature, and while the spectrum of fluctuations may become complicated, the average fluctuation rate is unlikely to drop much below the average rate just below the ordering temperature. Below T_N, the μSR signal continues to be relaxing from nearly full initial asymmetry, with no evidence of a unique ordered state magnetic field at the muons (that is, there is no hint of coherent precession of the muon polarization about such a field). This suggests a complicated antiferromagnetic ordering, such as has been seen in $NdRh_4B_4$ and $TmRh_4B_4$,[30] which would cause an apparently random distribution of fields at the muon site(s) different than the paramagnetic state distribution. In the ordered state of $SmRh_4B_4$ a two-exponential spin relaxation reminiscent of paramagnetic $ErRh_4B_4$ suddenly appears. Perhaps magnetostriction makes the RhB-cluster site more attractive, or perhaps one crystallographic site becomes two sites with respect to the magnetic ordering structure (though this is difficult to reconcile with the apparent disorder of the field distribution at each of the two sites). With the ordered state signal fully resolved (there is no missing signal), the μSR signal can evolve smoothly from the paramagnetic toward the ordered in the "critical regime" and need not "diverge." Some researchers, however, do prefer to continue fitting diverging equations to their data near transition temperatures even when the data merely peaks at the transition,[31] when theory predicts divergence.

If we assume that the rms component field at the muon does not change much as the magnetic ordering temperature is approached from above, then we can call the excess relaxation "excess slowing down" as a function of

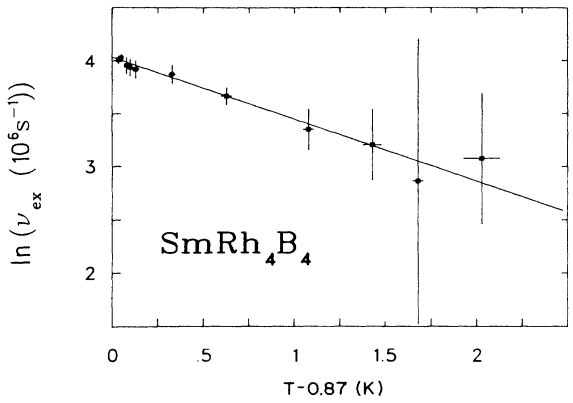

FIG. 10. Logarithm of "excess slowing down" of fluctuation rate in $SmRh_4B_4$ versus $T-T_N$ (where $T_N=0.87$ K). Best-fit straight line is shown.

temperature. Phenomenologically, this fits very well to an exponential (nondiverging) form:

$$\nu_{ex}=\nu_{T_+}\exp[-D(T-T_N)] \tag{18}$$

where ν_{T_+} is the limiting rate as the temperature approaches T_N from above, and D is the decay constant. This is shown by a plot of $\ln(\nu_{ex})$ versus $T-T_N$ in Fig. 10. The deduced ν_{T_+} is $(56\pm1)\times10^6$ s^{-1}, the deduced decay constant is 0.58 ± 0.08 K^{-1}. Any similar calculation involving a changing field distribution at the muon site would require a detailed model of the field distribution as a function of temperature (see, for an example, Ref. 32), which should be part of the application of a theory of the critical behavior of an antiferromagnetic superconductor, which we have not attempted at this time.

VI. CONCLUSIONS

Zero-field μSR in the RRh_4B_4 materials has proven to be rich in phenomenology. In this paper we have shown that the μSR data in $SmRh_4B_4$ and $ErRh_4B_4$, which at first appear so different, can be consistently interpreted in terms of well-known rare-earth spin-fluctuation mechanisms at all temperatures at which the signal is well resolved in $ErRh_4B_4$ and down to 4 K in $SmRh_4B_4$. From 4 K down to T_N in $SmRh_4B_4$ there is excess relaxation that seems associated with the magnetic ordering. This excess relaxation may be due to critical slowing down of the samarium moment fluctuations and/or to increasing average field magnitude at the muon as short-range order develops above the long-range ordering transition.

ACKNOWLEDGMENTS

The authors wish to thank R. Keitel, M. Senba, K. M. Crowe, and S. S. Rosenblum for help with the data-collecting equipment, M. B. Maple, S. E. Lambert, and M. S. Torikachvili for providing the samples, F. J. Rotella for giving us a copy of the ORTEP code and A. Boland for help with the site-modelling software. Work by D. R. Noakes, J. H. Brewer, D. R. Harshman, and E. J. Ansaldo was supported by the Canadian Natural Sciences and Engineering Research Council, and work by C. Y. Huang by the U. S. Department of Energy. TRIUMF is supported by the National Research Council of Canada.

*Present address: AT&T Bell Laboratories, 600 Mountain Ave., Murray Hill, NJ.

[1]For a review of the properties of this series, see M. B. Maple, H. C. Hamaker, and L. D. Woolf, in *Superconductivity in Ternary Compounds,* edited by M. B. Maple and Ø. Fischer (Springer, New York, 1982), Vol. 2, p. 99.

[2]T. Jarlborg, A. J. Freeman, and T. J. Watson-Yang, Phys. Rev. Lett. **39**, 1032 (1977).

[3]For an introduction to the RKKY interaction in rare-earth magnetism, see K. N. R. Taylor, Adv. Phys. **20**, 551 (1971).

[4]See, for example, L. D. Woolf, Phys. Lett. **93A**, 419 (1983).

[5]B. D. Dunlap, L. N. Hall, F. Behroozi, G. W. Crabtree, and D. G. Niarchos, Phys. Rev. B **29**, 6244 (1984); H. B. Radousky, B. D. Dunlap, G. S. Knapp, and D. G. Niarchos, *ibid.* **27**, 5526 (1983); H. B. Radousky, A. T. Aldred, G. S. Knapp, and J. S. Kouvel, *ibid.* **27**, 4236 (1983).

[6]K. Kumagai and F. Y. Fradin, Phys. Rev. B **27**, 2770 (1983); K. Kumagai, Y. Honda, and F. Y. Fradin, in *Proceedings of the 17th International Conference on Low-Temperature Physics,* edited by U. Eckern, A. Schmid, W. Weber, and H. Wuhl (Elsevier, Amsterdam, 1984), p. 93.

[7]R. H. Heffner, D. W. Cooke, R. L. Hutson, M. E. Schillaci, J. L. Smith, P. M. Richards, D. E. MacLaughlin, S. A. Dodds, and J. Oostens, J. Appl. Phys. **57**, 3107 (1985); R. H. Heffner, D. W. Cooke, R. L. Hutson, M. Leon, M. E. Schillaci, J. L. Smith, A. Yaouanc, S. A. Dodds, L. C. Gupta, D. E. MacLaughlin, and C. Boekema, *ibid.* **55**, 2007 (1984); D. E. MacLaughlin, S. A. Dodds, C. Boekema, R. H. Heffner, R. L. Hutson, M. Leon, M. E. Schillaci, and J. L. Smith, J. Magn. Magn. Mater. **31-34**, 497 (1983); C. Boekema, R. H. Heffner, R. L. Hutson, M. Leon, M. E. Schillaci, J. L. Smith, S. A. Dodds, and D. E. MacLaughlin, J. Appl. Phys. **53**, 2625 (1982).

[8]C. Y. Huang, E. J. Ansaldo, J. H. Brewer, D. R. Harshmann, K. M. Crowe, S. S. Rosenblum, C. W. Clawson, Z. Fisk, S. E. Lambert, M. S. Torikachvili, and M. B. Maple, Hyperfine Interact. **17-19**, 509 (1984).

[9]D. R. Noakes, E. J. Ansaldo, J. H. Brewer, D. R. Harshman, C. Y. Huang, M. S. Torikachvili, S. E. Lambert, and M. B. Maple, J. Appl. Phys. **57**, 3197 (1985).

[10]R. S. Hayano, Y. J. Uemura, J. Imazato, N. Nishida, T. Yamazaki, and R. Kubo, Phys. Rev. B **20**, 850 (1979).

[11]J. H. Brewer, Hyperfine Interact. **8**, 831 (1981).

[12]R. Kubo, J. Phys. Soc. Jpn. **9**, 935 (1954).

[13]E. Holzschuh, and P. F. Meier, Phys. Rev. B **29**, 1129 (1984).
[14]Y. J. Uemura, Ph.D. thesis, University of Tokyo, 1982 (unpublished).
[15]K. Kumagai, Y. Inoue, Y. Kohori, and K. Asayama, in *Ternary Superconductors,* edited by G. K. Shenoy, B. D. Dunlap, and F. Y. Fradin (Elsevier/North-Holland, New York, 1981), p. 185.
[16]Y. Kohori, M. Matsumara, T. Kohara, K. Kumagai, and K. Asyama, J. Magn. Mag. Mater. **31-34**, 495 (1983).
[17]T. Matsuzaki, K. Nishiyama, K. Nagamine, T. Yamazaki, M. Senba, J. M. Bailey, and J. H. Brewer (unpublished).
[18]R. Kubo and T. Toyabe in *Magnetic Resonance and Relaxation,* edited by R. Blinc (North-Holland, Amsterdam, 1967), p. 810; and D. R. Harshman, Ph.D. thesis, University of British Columbia, 1986 (unpublished).
[19]D. R. Noakes, Proceedings of the 4th International Conference on μSR, 1986 [Hyperfine Interact. **31**, 47 (1986)].
[20]K. J. Standley and R. A. Vaughan, *Electron Spin Relaxation Phenomena In Solids* (Hilger, London, 1969).
[21]C. Y. Huang, Phys. Rev. **139**, A241, (1965).
[22]H. Zhou, J. W. Chen, S. E. Lambert, and M. B. Maple, J. Appl. Phys. **57**, 3115 (1985).
[23]H. Zhou, S. E. Lambert, M. B. Maple, B. D. Dunlap, and S. K. Malik (unpublished).
[24]See, for example, C. Y. Huang and N. L. Huang-Liu, in *Crystalline Electric Field and Structural Effects in f-Electron Systems* edited by J. E. Crow, R. P. Guertin, and T. W. Mihalisin (Plenum, New York, 1980), p. 465.
[25]S. B. Woods (private communication).
[26]H. Hasegawa, Prog. Theor. Phys. **21**, 483 (1959).
[27]M. R. McHenry, B. G. Silbernagel, and J. H. Wernick, Phys. Rev. B **5**, 2958 (1972).
[28]See, for example, H. R. Kirchmayr, and C. A. Poldy, in *Handbook on the Physics and Chemistry of Rare Earths,* edited by K. A. Gschneidner and L. Eyring (North-Holland, Amsterdam, 1979), Vol. 2, p. 55.
[29]R. S. Hayano, Y. J. Uemura, J. Imazato, N. Nishida, T. Yamazaki, H. Yasuoka, and Y. Ishikawa, Phys. Rev. Lett. **41**, 1743 (1978).
[30]C. F. Majkrzak, D. E. Cox, G. Shirane, H. A. Mook, H. C. Hamaker, H. B. MacKay, Z. Fisk, and M. B. Maple, Phys. Rev. B **26**, 245 (1982); C. F. Majkrzak, S. K. Satija, G. Shirane, H. C. Hamaker, Z. Fisk, and M. B. Maple, *ibid.* **27**, 2889 (1983).
[31]See, for example, K. Sugawara, C. Y. Huang, and D. L. Huber, J. Low Temp. Phys. **26**, 525 (1977).
[32]E. Wackelgard, O. Hartmann, E. Karlsson, R. Wappling, J. Chappert, A. Yaouanc, L. Asch, and G. M. Kalvius, Proceedings of the 4th International Conference on μSR, 1986 [Hyperfine Interact. **31**, 325 (1986)].